ELSEVIER

NeuroImage

www.elsevier.com/locate/ynimg
NeuroImage 31 (2006) 66 – 75

Blood volume and hemoglobin oxygenation response following electrical stimulation of human cortex

Minah Suh, Sonya Bahar,[1] Ashesh D. Mehta, and Theodore H. Schwartz*

Department of Neurosurgery, Weill Cornell Medical College, New York Presbyterian Hospital, 525 East 68th St., Box #99, New York, NY 10021, USA

Received 14 June 2005; revised 23 September 2005; accepted 18 November 2005
Available online 15 February 2006

Our understanding of perfusion-based human brain mapping techniques relies on a detailed knowledge of the relationship between neuronal activity and cerebrovascular hemodynamics. We performed optical imaging of intrinsic signals at wavelengths sensitive to total hemoglobin (Hbt; which correlate with cerebral blood volume (CBV)) and deoxygenated hemoglobin (Hbr) directly in humans during neurosurgical operations and investigated the optical signals associated with bipolar cortical stimulation at a range of amplitudes. Cortical stimulation elicited a rapid focal increase in Hbr (initial dip) in all subjects. An equally rapid increase in Hbt (<200 ms), with a slightly higher signal-to-noise ratio, was also highly localized for <2 s in spite of the non-columnar nature of the stimulus, after which the signal spread to adjacent gyri. A later decrease in Hbr (>3 s), which is relevant to the blood oxygen level dependent (BOLD) signal, was poorly localized. Increasing the stimulus amplitude elicited a linear increase in the area of the optical signal for Hbt and the initial dip but not the late decrease in Hbr, and a nonlinear increase in optical signal amplitude with a plateau effect for initial dip, Hbt and late decrease in Hbr.

Introduction

The field of human brain mapping has undergone a revolution in the past 10 years as a result of technical advances in high-resolution perfusion/oxygenation-based techniques such as fMRI and optical recording of intrinsic signals (ORIS). Both techniques are based on the work of Roy and Sherrington (1890) who observed a coupling between electrical activity and cerebral blood flow (CBF) in the microcirculation (Roy and Sherrington, 1890). More recently, Fox and Raichle (1986) demonstrated that increases in CBF, which occur 1–2 s after the neurons become active, are far greater than increases in metabolic demand ($CMRO_2$) (Fox and Raichle, 1986; Fox et al., 1988). This mismatch leads to an increase in oxygenated hemoglobin (HbO_2), which causes a relative decrease in the concentration of Hbr and is the basis of the BOLD signal seen with fMRI (Ogawa et al., 1990). It is still controversial whether the increase in $CMRO_2$ causes a transient focal increase in deoxygenated hemoglobin (Hbr) in the first few hundred milliseconds after the neurons become active (Devor et al., 2003; Forsting et al., 1993; Frostig et al., 1990; Nemoto et al., 1999; Sheth et al., 2003; Malonek and Grinvald, 1996; Ernst and Henning, 1994; Mayhew et al., 1999; Vanzetta and Grinvald, 1999; Menon et al., 1995;Hu et al., 1997; Kim et al., 2000; Lindauer et al., 2001; Logothetis et al., 1999; Frannson et al., 1998; Mandeville et al., 1999; Silva et al., 2000). Critics contend that this "initial dip" is an epiphenomenon of the experimental method, based on species, level of anesthesia, data analysis method or merely secondary to changes in blood volume (Buxton, 2001; Buxton et al., 1998; Lindauer et al., 2001).

The putative existence of this early increase in Hbr is of critical importance. As a mapping signal, the early $CMRO_2$-related increase in Hbr may have a more precise spatial correlation with the population of active neurons than the later CBF-related decrease in Hbr that forms the basis of the BOLD mapping signal. One hypothesis for the inconsistent presence of the initial dip is based on a theoretical tissue oxygen buffer (Buxton et al., 1998). In this model, activation of a small population of neurons may not sufficiently increase $CMRO_2$ to affect an increase in Hbr, whereas higher levels of activation will overcome the buffer. In support of this theory, Suh et al. (2005) recently demonstrated a large increase in Hbr following epileptiform events, in which enormous populations of neurons are simultaneously active.

Another potential mapping signal arises from very early activity-related increases in cerebral blood volume (CBV), which were initially thought to be less localizing than the initial dip (Frostig et al., 1990; Malonek and Grinvald, 1996). Recent animal data, however, have shown that increases in CBV may be highly localized within the first 2 s after the electrophysiological event, potentially offering a better signal-to-noise ratio than the initial dip

* Corresponding author. Fax: +1 212 7465592.
E-mail address: schwarh@med.cornell.edu (T.H. Schwartz).
[1] Present address: Center for Neurodynamics, Department of Physics and Astronomy, University of Missouri at St. Louis, St. Louis, MO, USA.
Available online on ScienceDirect (www.sciencedirect.com).

1053-8119/$ - see front matter © 2005 Elsevier Inc. All rights reserved.
doi:10.1016/j.neuroimage.2005.11.030

(Sheth et al., 2003; Erinjeri and Woolsey, 2002; Hess et al., 2000; Nemoto et al., 2004; Sheth et al., 2004). Although as a mapping signal, its utility may depend on the columnar distribution of microvascular modules (Sheth et al., 2004; Vanzetta et al., 2004; Woolsey et al., 1996).

Our understanding of the spatiotemporal dynamics of perfusion and oxygenation associated with neuronal activity arises mainly from animal experiments on normal sensory processing of columnar activity. Whether these data apply to the human brain and to non-columnar activity is unclear since techniques with sufficient resolution to address these questions, such as ORIS or oxygen-sensitive electrodes, are invasive and difficult to perform on the human brain for both technical and ethical reasons.

The recent implementation of ORIS in the neurosurgical operating room for human brain mapping has generated a great deal of excitement since it potentially has the highest combined spatial and temporal resolution of any human imaging technique (Cannestra et al., 2001; Cannestra et al., 1998; Haglund et al., 1992; Pouratian et al., 2003; Sato et al., 2002a; Shoham and Grinvald, 2001; Haglund and Hochman, 2004). At isosbestic wavelengths of hemoglobin where HbO_2 and Hbr reflect light equally (525, 545, 570.5 and 583 nm) (Sheth et al., 2003), ORIS measures total hemoglobin (Hbt), which is directly proportional to CBV and CBF assuming that the concentration of red blood cells remains constant (Nemoto et al., 2004; Mayhew et al., 2000). At higher wavelengths (600–650 nm), the majority of the signal arises from the oxygenation state of hemoglobin since Hbr absorbs light with three times the absorption coefficient of HbO_2 (Malonek and Grinvald, 1996; Sato et al., 2002b) Hence, a decrease in light reflection indicates an increase in Hbr. With multiwavelength imaging and a modified Beer–Lambert law calculation, it is possible to directly calculate Hbr, HbO_2 and Hbt.

Several groups have reported intraoperative single wavelength imaging of intrinsic signals, ranging from 605 to 695 nm, in response to sensory and epileptiform events, with little investigation into the spatial specificity of the various components of the intrinsic signal (Cannestra et al., 1998; Haglund and Hochman, 2004; Haglund et al., 1992; Pouratian et al., 2003; Sato et al., 2002a; Shoham and Grinvald, 2001). Optical responses have generally been monophasic with little evidence or mention of an initial dip. We used the opportunity provided by patients with epilepsy who are undergoing a craniotomy for implantation of subdural electrodes to investigate the spatiotemporal dynamics of perfusion and oxygenation associated with the activation of graded populations of neurons using multiwavelength ORIS. We chose to activate the cortex with bipolar cortical stimulation since this form of direct cortical stimulation produces highly localized current flow in a non-columnar distribution, exciting nearly 90% of adjacent cells with rapid spatial fall-off, and the number of responding cells varies directly with the amplitude of stimulation, with a plateau effect (Butovas and Schwarz, 2003; Nathan et al., 1993).

Methods

Subjects

Eight patients undergoing craniotomy for resection of medically intractable epilepsy gave consent for the imaging procedure described below, which was approved by the Institutional Review Board at Weill Cornell Medical Center. Most patients had undergone a prior craniotomy for implantation of electrodes to record interictal and ictal electrographic data and for stimulation mapping of motor, sensory, and language cortex. Hence, prior to ORIS, the location of the seizure focus as well as surrounding functional cortex was known. ORIS was performed during a second operation when electrodes were removed from the brain, just prior to resective surgery. ORIS was performed under general anesthesia consisting of isoflurane (<0.2%) and remyfentanyl (1 μg/kg/h). All other anesthetic agents were discontinued 20 min prior to the start of the experiment.

Electrical stimulation and recording

Two 4-contact strip electrodes (interelectrode distance—1 cm; Ad-Tech, Madison, WI) were placed on surface of the brain adjacent to one another (Fig. 1B). The two distal contacts of one strip were used for electrical stimulation, while the two distal contacts of the second strip were used to record surface potentials from an adjacent gyrus (Fig. 1B). The use of two separate strips allowed for maximal flexibility in choosing the site of stimulation and recording. Stimulation was performed on the crest of a gyrus, either within the epileptic focus (4 subjects) or in an adjacent brain (4 subjects) in either the parietal or frontal lobe, at least 1 cm from the Sylvian fissure or other large superficial veins. The epileptic focus was defined as areas of ictal onset or interictal spiking during chronic recordings from the surface of the brain with implanted electrodes. Stimulation outside of this area was considered "adjacent" brain.

Bipolar stimulation was delivered either from an Ojemann Stimulator (Integra Neurosciences) or an S-12 stimulator (Grass-Telefactor), triggered by the ORIS computer. Biphasic trains of 1 ms pulses were delivered at 60 Hz for 2 or 3 s at amplitudes of 1 to 4 mA. The amplitude and stimulation lengths were similar to parameters used during electrical stimulation mapping of the human brain for neurosurgical procedures (Ojemann, 1991). Parameters remained constant within a given experiment.

Electrocorticography data were amplified (Grass 1P511) and digitized at 2000 Hz (CED Power 1401, Cambridge, UK) and recorded onto a PC using Spike 2 (Cambridge Electronic Design, Cambridge, UK). Online examination was performed to ensure the absence of afterdischarges and spreading depression for each trial (Fig. 1D). Recordings looked similar for all non-rejected stimulation trials, and therefore other examples are not shown. The EKG was taken directly from the anesthesia machine and digitized onto a PC and recorded with an oscilloscope (BK Precision, 2120B) and window discriminator (FHC) to trigger the ORIS acquisition computer.

Optical imaging

A sterile glass footplate (4 × 4 cm) was placed on the surface of the brain over the electrodes for stabilization and to dampen the movement artifacts caused by heartbeat and respiration. A custom-made camera holder with gross and fine $x-y-z$ manipulators was used to suspend the camera over the surface of the brain (Imager 3001D—analog camera, Optical Imaging Inc., Germantown, NY) (Fig. 1A). A single 35 mm lens was used for image acquisition since a back-to-back lens system did not provide an adequate field of view (Schwartz et al., 2004; Ratzlaff and Grinvald, 1991). We performed 3 × 3

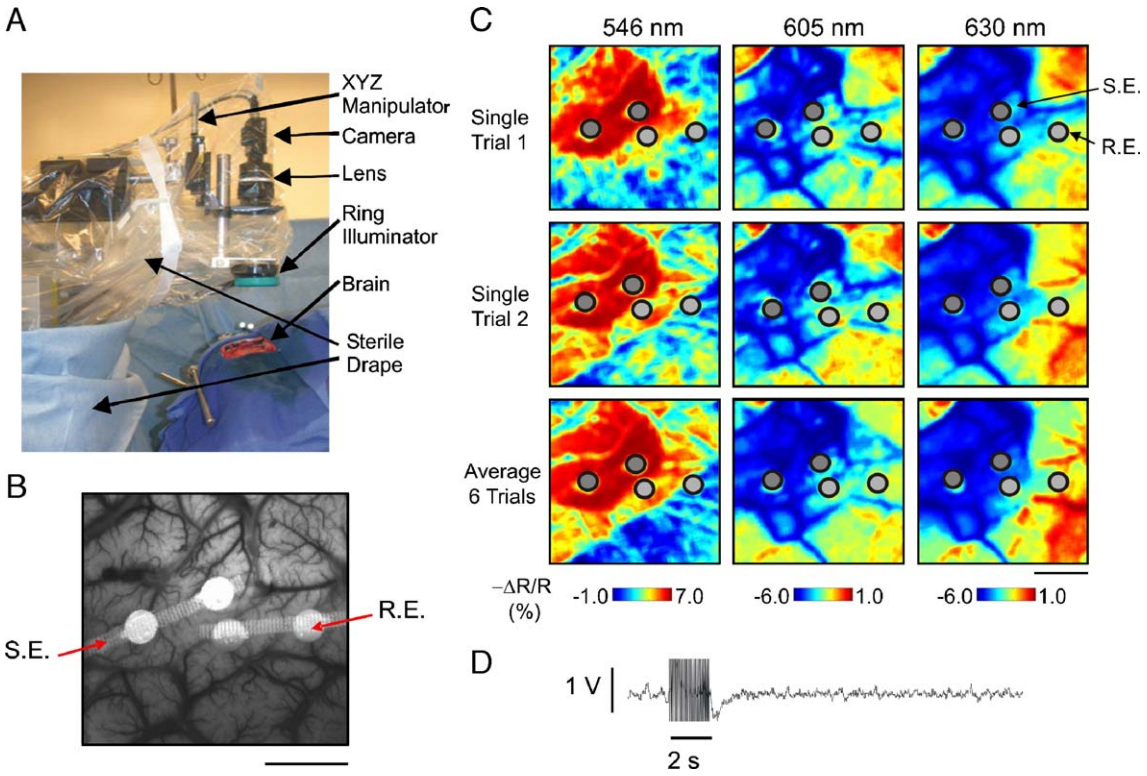

Fig. 1. Experimental set-up and reproducibility of the stimulus-induced optical signal. (A) A custom camera holder with $x-y-z$ gross and fine manipulators suspends a camera, lens, and ring illuminator, draped in sterile plastic, over the exposed human cortex. (B) Two strip electrodes are placed on the surface of the brain, a stimulating electrode (S.E.) and a recording electrode (R.E.). The surface of the brain is stabilized with a glass footplate. Image acquired at 546 nm. Scale bar: 1 cm. (C) At 6 s following stimulation at 3 mA, the optical signal derived from two separate individual trials is nearly identical to the signal averaged over 6 trials, at 546 nm, 605 nm, and 630 nm. At this moment in time, the signal at 546 nm reveals an increase in Hbt around the stimulating electrodes, while the images at 605 and 630 reveal changes in the concentration of Hbr, in a similar location. Notice that the image acquired at 605 nm is nearly identical to the image acquired at 630 nm. The locations of the stimulating and recording electrodes are indicated with gray circles. Scale bar: 1 cm. (D) The electrocorticography recordings reveal a 2-s stimulus artifact and the absence of afterdischarges or spreading depression.

binning of the 768 × 480 pixel resolution to reduce the size of each dataset. The operating room was darkened and the cortex illuminated with a ring illuminator attached to Tungsten halogen lamp (100 W). The light was passed through bandpass filters of different wavelengths, first at 546 ± 10 nm to record the surface blood vessel pattern and then at 546 ± 10 nm and either 605 ± 10 nm or 630 ± 10 nm, or both 605 ± 10 and then 630 ± 10 nm following electrical stimulation. We chose the investigate Hbr at two separate wavelengths since earlier studies in animals were done at wavelengths ranging from 605 to 630 nm (Sheth et al., 2003; Vanzetta et al., 2004; Ratzlaff and Grinvald, 1991), and we wished to determine if this difference would affect the signal in humans. The optical reflectance signal was digitized onto a PC at 33 frame/s and integrated at variable frame rates from 2 to 10 Hz, which were kept constant during a given experiment. We used 2 Hz to examine the time course of the signal throughout the trial and 10 Hz to measure the latency of onset of the signal immediately after stimulation.

Experiments consisted of 6–12 trials of cortical stimulation at each amplitude, delivered in nonrandom order. In some experiments, low amplitude stimulation was given first, and, in other experiments, high amplitude stimulation was first, which had no influence on the results. Image acquisition began simultaneously with electrical stimulation. The interstimulus interval was 44 s. Imaging at each wavelength was performed sequentially, but the order was varied between experiments.

Data analysis

Pixel values of the raw data for each trial were measured. We noted periodic, random, non-stimulus-related fluctuations in cortical reflectance with an amplitude of 5–8%. Trials with this large "vasomotor noise" were eliminated. In general, only 1 or 2 trials per subject were eliminated due to this noise, which has a periodicity of 0.1 Hz in animals (Mayhew et al., 1996) but is more irregular in humans (0.1–0.2 Hz) (Shoham and Grinvald, 2001). Stimulus-related changes in the amplitude of light reflectance were appreciated by dividing each frame acquired after cortical stimulation by the frame acquired at the onset of stimulation and then averaged over all trials of the same amplitude and wavelength. Since the ORIS signal following electrical stimulation is so large, the signal-to-noise ratio is sufficiently high that little averaging is required. In fact, a single trial was usually adequate to generate reasonable data, although we always used averaged data in our analysis to increase the signal-to-noise ratio. Change in reflection of light was calculated as $-\Delta R/R$ (%) from multiple regions of interest using custom-written software (Matlab, The Mathworks). Images were filtered with a moving 5 × 5 vector for smoothing for presentation in figure form. The signal-to-noise ratio was calculated by dividing the amplitude of the signal at its maximum by the amplitude of the variations in the optical signal during the last 5 s of the control or "no stimulus" trial. The area of activation was calculated based on statistically significant

changes in light reflection for each pixel according to the following methods. Pixels with a change in reflection beyond 3 SD above or below the mean compared with baseline were considered significant. Baseline was defined from an ROI measured between the stimulating electrodes prior to cortical stimulation.

Spectroscopic calculations and terminology

Recordings at 546 nm, an isosbestic wavelength for hemoglobin, measure Hbt. Since Hbt is proportional to CBV, if the hematocrit remains constant, we refer to the optical signal at this wavelength as CBV. Optical recordings at 605 and 630 nm are not a pure measure of Hbr since this wavelength is also sensitive to HbO_2, albeit less so than Hbr, and thus can theoretically be contaminated by large increases in CBV. Hence, the concentration of Hbr must be calculated using a modified form of the Beer–Lambert law which described light attenuation in the presence of absorbance and scattering:

$$\log\frac{I_o^{\lambda}}{I(T)} = \left(\varepsilon_{\mathrm{Hbr}}^{\lambda}\Delta[\mathrm{Hbr}](t) + \varepsilon_{\mathrm{HbO_2}}^{\lambda} \times \Delta[\mathrm{HbO_2}](t)\right) \times l^{\lambda} + \Delta S \quad (1)$$

where I_o is the pre-stimulus intensity, $I(t)$ the measured intensity time course, ε extinction coefficients, l the pathlength through the tissue, S scattering, $\Delta[\mathrm{Hbr}](t)$ and $\Delta[\mathrm{HbO}^2](t)$ is the time course of change in absorbers, and superscript λ indicates wavelength dependency. By measuring I_o and $I(t)$ at two wavelengths and using the known wavelength dependency of the optical path length ($\alpha = \varepsilon \times l$) (Sheth et al., 2004), we determine a pathlength corrected value of $\Delta[\mathrm{Hbr}](t)$ and $\Delta[\mathrm{HbO_2}](t)$. Wavelength dependency of the optical path length was drawn from work by Sheth et al. using an in vitro phantom (Sheth et al., 2004, Fig. 1).

Results

Reproducibility of intrinsic signal changes following cortical stimulation

After eliminating trials with afterdischarges or significant vasomotor noise, we found that bipolar stimulation of the human cortex elicited an extremely reliable and reproducible optical signal, regardless of the wavelength of incident light (Fig. 1C). Our data could not be confused with vasomotor noise since the signals were temporally linked to electrical stimulation; furthermore, no evidence of spreading depression was observed on the recording electrodes. Two-dimensional cross correlations between images from individual trials were highly significant, regardless of wavelength ($r = 0.76$, $P < 0.01$). Images recorded at 605 nm were nearly identical with images recorded at 630 nm ($r = 0.85$, $P < 0.01$), and so the data recorded at these two separate wavelengths were pooled for further analysis (Fig. 1C). All electrical recording traces appeared similar, showing a stimulus artifact for the duration of the stimulation followed by a brief surface negativity (Fig. 1D). This is consistent with the known effects of epicortical stimulation, namely, a burst of excitatory activity followed by a period of inhibition (Butovas and Schwarz, 2003; Creutzfeldt et al., 1966).

Amplitude, time course, and spatial spread of CBV and Hbr

The intrinsic signal measured from a region of interest (ROI) between the stimulating electrodes recorded at 546 nm was monophasic (Fig. 2), and the mean (SD) maximal signal, measured as $-\Delta R/R$ (%), was 12.7 ± 5.3% (averaged among subjects recorded within the epileptic focus (EF)), 7.47 ± 3% (averaged among subjects recorded outside the epileptic focus (OF)), and 9.7 ± 5% for all subjects (AS). At wavelengths sensitive to Hbr, the intrinsic signal was clearly biphasic (Fig. 2). Early, within the first 1–2 s after

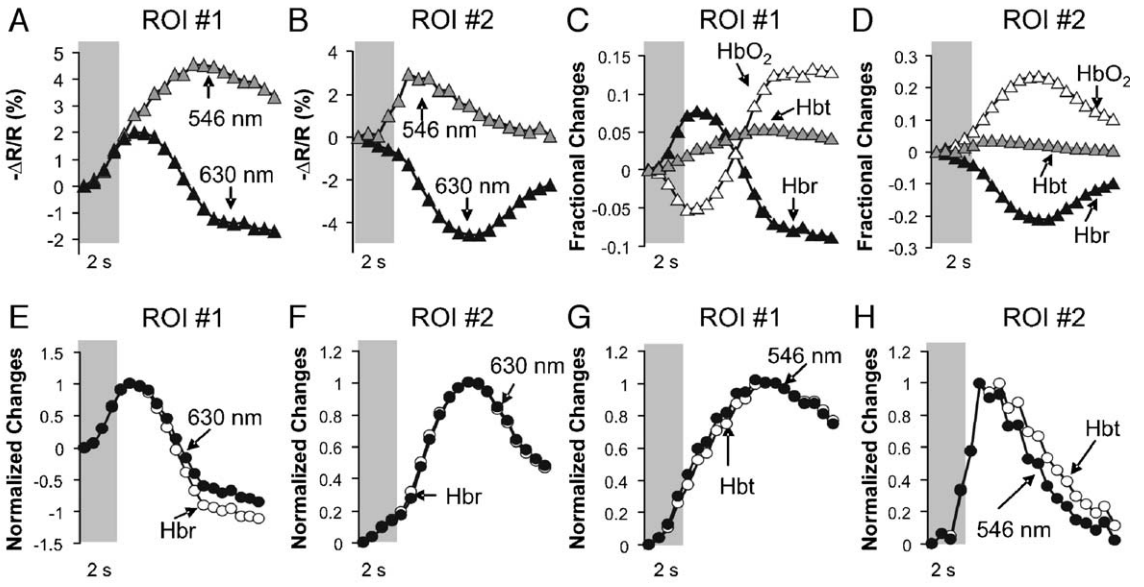

Fig. 2. Time course of intrinsic signal recorded at 546 nm and 630 nm and calculated Hbr, HbO_2, and Hbt. (A and B) Time course of intrinsic signal recorded at 546 nm and 630 nm from ROI_1 (A) and ROI_2. (B) from Fig. 3A. (C and D) Time course of calculated Hbr, HbO_2, and Hbt signals at ROI_1 (C) and ROI_2 (D). (E and F) Normalized time course of 630 nm and Hbr from ROI_1 (E) and ROI_2 (F). Similar temporal profiles and peak magnitude coupling suggest high correlation between recorded intrinsic signal and calculated Hbr. (G and H) Normalized time course of 546 nm and Hbt from ROI_1 (G) and ROI_2 (H). Changes in Hbt reflect changes in intrinsic signal recorded at 546 nm. Gray bar marks duration of cortical stimulation.

stimulation, a decrease in reflection was recorded between the stimulating electrodes with a $-\Delta R/R$ (%) of 2.7 ± 1.5% (EF), 4 ± 1.8% (OF), and 3.5 ± 1.7% (AS). The signal-to-noise ratio of this early increase was 3.6, which was significantly smaller than the intrinsic optical signal recorded at 546 nm (6.7) ($P < 0.05$), which is comparable to that obtained in laboratory animals (Nemoto et al., 2004). Since there was no significant difference between signals recorded within or outside the focus, the two results were averaged together for the rest of the paper.

Using a modified Beer–Lambert law with pathlength correction, we calculated Hbr, HbO_2, and Hbt. Early increases in Hbr and decreases in HbO_2 were seen in all patients. The maximum Hbr and minimum HbO_2, measured as a fractional change (mean ± SD), was 0.14 ± 0.06 and −0.09 ± 0.04 respectively. In contrast, a more gradual increase in Hbt (proportional to CBV) peaked ~6 s after stimulation with a maximal fractional changes of 0.10 ± 0.04. At this very late time point, the signal had spread far beyond the stimulating electrodes to adjacent gyri (Fig. 3). The mean area of spread of Hbt was 164.63 ± 119.96 mm^2.

The area of spread of Hbr signal, on the other hand, was 77.16 ± 35.11 mm^2, which was more focal than the Hbt signal at its maximum (Fig. 3D). On average, after 2–3 s, the Hbr signal inverted indicating a decrease in Hbr, which is relevant to the BOLD signal. However, persistent focal decreases in Hbr could be seen for as long as 8 s in certain patients, particularly, with higher levels of stimulation (Figs. 3 and 4). The amplitude of this late Hbr signal was −0.32 ± 0.13, and the signal-to-noise ratio was 8.7. The area of the later decrease in Hbr was largest, reaching 349.05 ± 200.97 mm^2 at its maximum and was centered around the large draining veins (Figs. 1C, 3B). The area of spread of this decrease in Hbr reached its maximum ~10 s. The relative amplitude of the initial dip to the late decrease in Hbr was 1:4.5. Hence, at their respective maxima, the area of spread of the decrease in Hbr was larger than the Hbt signal, which was larger than the initial dip (ANOVA, $P < 0.02$). Of note, images recorded at 546 nm were significantly correlated with images of Hbt ($r > 0.86$, $P < 0.01$) as were images recorded at either 605 or 630 nm with Hbr images ($r > 0.89$, $P < 0.01$). Hence, the Beer–Lambert correction did not significantly change the raw optical signals. For this reason, uncorrected images are presented in Fig. 4.

Latency and spatial specificity of "very early" intrinsic signal

In order to determine the latency of the Hbt- and Hbr-related optical signal, we measured the intrinsic signal changes with a frame rate of 10 Hz in a subset of patients ($n = 4$). A statistically significant change in reflection was measured as early as 200 ms at 546 nm, at 100 ms at 605 nm, after stimulation (Fig. 4B). Such a rapid change in reflection is also seen after epileptiform events in animal models (Suh et al., 2005). At 1 s after stimulation, the area

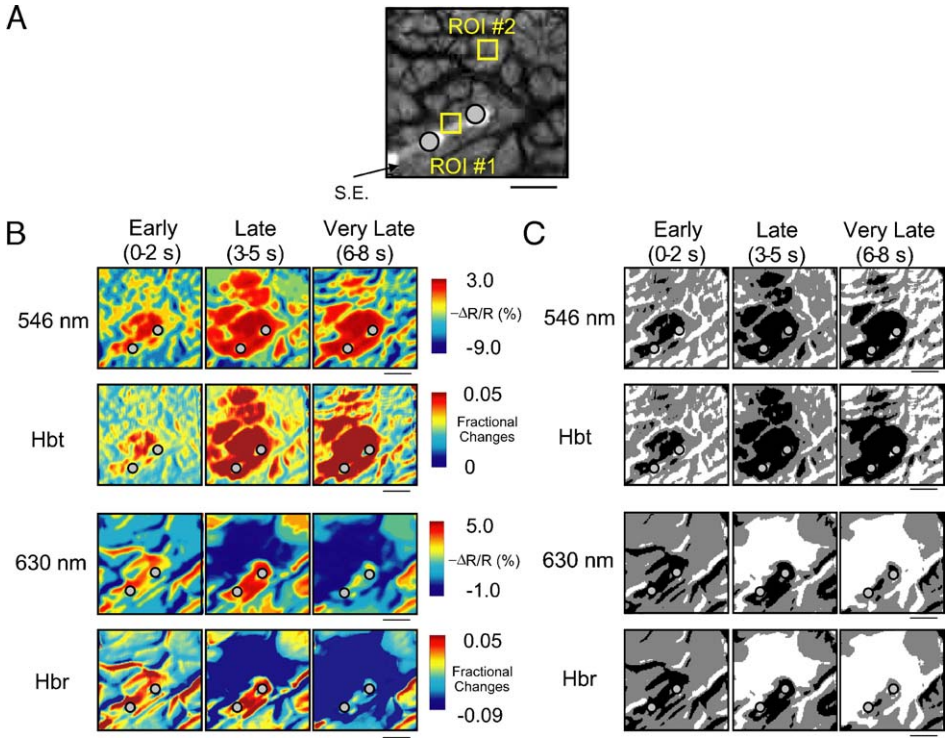

Fig. 3. The "initial dip" in hemoglobin oxygenation occurs earlier and more focally than CBV. (A) Surface of the brain with stimulating electrode (S.E.) under glass footplate at 546 nm. The recording electrode is outside the field of view. The yellow boxes are ROIs from which the data in Fig. 2 are taken. ROI_1 sits between the stimulating electrodes, and ROI_2 sits over an adjacent gyrus. Scale bar: 1 cm. (B) Intrinsic signal recorded at 546 and 630 nm at varying latencies after stimulation shows that, although the amplitude of the signal at 546 nm is larger than at 630 nm, the initial changes in signal recorded at 630 nm are more focal than the change in signal recorded at 546 nm, even within the first 2 s after stimulation. Images recorded at 546 nm and 630 nm were nearly identical with calculated Hbt and Hbr images ($r = 0.89$, $P < 0.05$). As time passes, the Hbt signal spreads diffusely throughout the cortex. At increasing latencies, a decrease in Hbr, consistent with the BOLD effect, appears in widespread cortical areas around the stimulating electrode as well as in the region of the "initial dip". (C) Statistically significant area of activation recorded at 546 and 630 nm and statistically significant area of calculated Hbt and Hbr images at different latencies after stimulation. The area of activation was determined based on statistically significant changes in light reflection for each pixel (3 SD above or below the baseline). Example is from a different patient than shown in Fig. 1. Location of stimulating electrodes shown with gray circles. Scale bar: 1 cm.

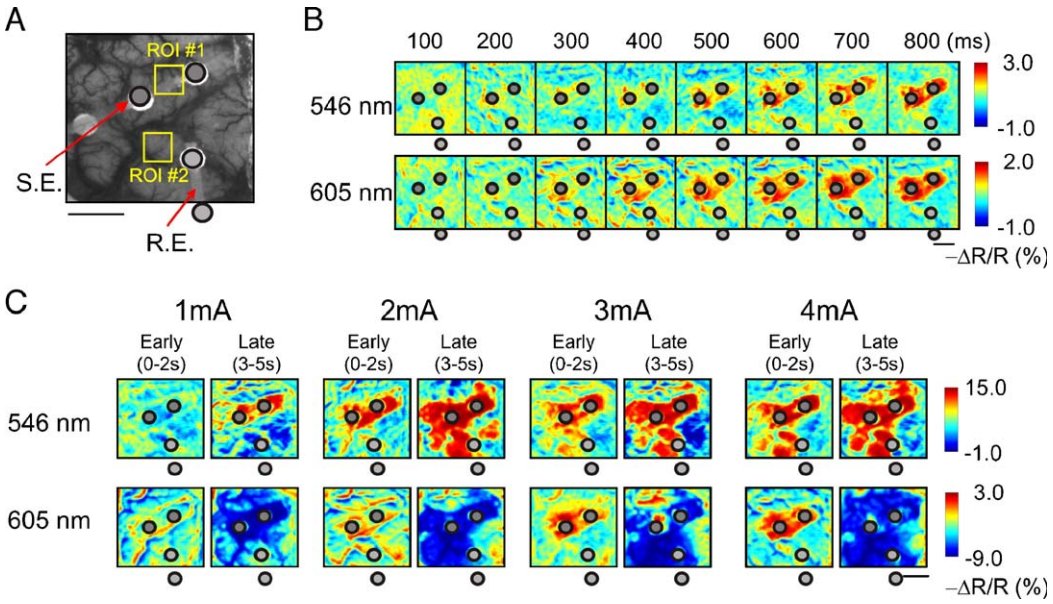

Fig. 4. Latency and amplitude dependence of intrinsic optical signals. (A) Cortical surface imaged at 546 nm shows locations of stimulating electrode (S.E.) and recording electrode (R.E.) in relation to surface vasculature. (B) Intrinsic signal recorded every 0.1 s shows a focal change in the amplitude of light reflectance at the site of the stimulating electrode starting ~0.2 s following cortical stimulation at both wavelengths. (C) Intrinsic signal at different time points following cortical stimulation at varying amplitudes reveals amplitude dependence of $-\Delta R/R$ (%) and area of spread of intrinsic signal. Gray circles indicate positions of stimulating and recording electrodes. Scale bars: 1 cm.

of spread of the intrinsic signal was 42.20 ± 38.37 mm^2 at 546 nm versus 47.35 ± 37.09 mm^2 at 605 nm (n.s.). Hence, at these very early time points, the intrinsic signal was highly localized to the region of cortical stimulation, regardless of wavelength. Nevertheless, the amplitude of the intrinsic signal at these very early time points was slightly larger at 546 nm (1.6 ± 0.6%) than at 605 nm (0.9 ± 0.4%).

Correlation between amplitude of electrical stimulation and intrinsic signal

We measured the intrinsic signal at each wavelength while varying the amplitude of cortical stimulation from 1 to 4 mA, in 1 mA increments (n = 3). Increasing the stimulus amplitude elicited an increase in both the area of spread and the change in the amplitude of light reflectance (Fig. 4C). A similar finding has been reported following hindlimb stimulation in rat (Sheth et al., 2003, 2004). The relationship between the stimulus amplitude and the area of spread was well approximated by a linear fit for both the late decrease in Hbr (BOLD-like signal) (r > 0.90) and the Hbt (r > 0.89) signals. The initial dip, however, fit best to a second order polynomial (r = 0.91; Fig. 5E). On the other hand, the relationship between the change in the amplitude of light reflectance and the stimulus amplitude was best fit with a second order polynomial for all signals, with a plateau effect (r > 0.90; Fig. 5F).

Discussion

We report the first measurements of deoxygenated hemoglobin in the human at such high spatial and temporal resolution. Although our data are derived from patients with epilepsy, neurosurgical operations for the treatment of disease currently provide the only access to the exposed human brain. We find that the initial dip in hemoglobin oxygenation is present at all stimulation amplitudes and is highly localized to the area of neuronal activity following direct cortical stimulation. In addition, within the first 1–2 s, the increase in Hbt is equally as focal as the initial dip and thus can provide another source for high-resolution cortical mapping in humans, even with non-columnar neuronal activity. At later time points (>3 s), the decrease in Hbr, which is relevant to the BOLD signal, and the Hbt signal are no longer localized to the region of electrophysiologic activation and involve several centimeters of surrounding cortex as well as adjacent gyri. However, the initial dip remains highly localized for the duration of its existence.

Although the initial dip has been demonstrated in several species with techniques including ORIS at wavelengths sensitive to Hbr (600–660 nm) (Nemoto et al., 1999; Devor et al., 2003; Frostig et al., 1990; Sheth et al., 2003), imaging spectroscopy (Malonek and Grinvald, 1996; Mayhew et al., 1999), oxygen-sensitive electrodes (Thompson et al., 2003, 2004; Ances et al., 2001), oxygen-dependent phosphorescence quenching (Vanzetta and Grinvald, 1999), and fMRI at 1.5 and 4-T (Ernst and Henning, 1994; Menon et al., 1995; Hu et al., 1997; Logothetis et al., 1999; Kim et al., 2000), there is ample evidence of an absence of an initial dip with these techniques and its existence remains controversial (Lindauer et al., 2001; Frannson et al., 1998; Mandeville et al., 1999; Silva et al., 2000; Sheth et al., 2004). Other explanations for inconsistent results point to the dependence of the initial dip on anesthetic techniques, pO_2, analysis algorithm, as well as stimulus and species dependence (Lindauer et al., 2001; Vanzetta and Grinvald, 2001). Another criticism has been that, since HbO_2 does absorb some light at wavelengths sensitive to hemoglobin oxygenation, large changes in Hbt might influence the optical signal and contaminate the data. However, laboratory studies in animals using oxygen-sensitive electrodes have con-

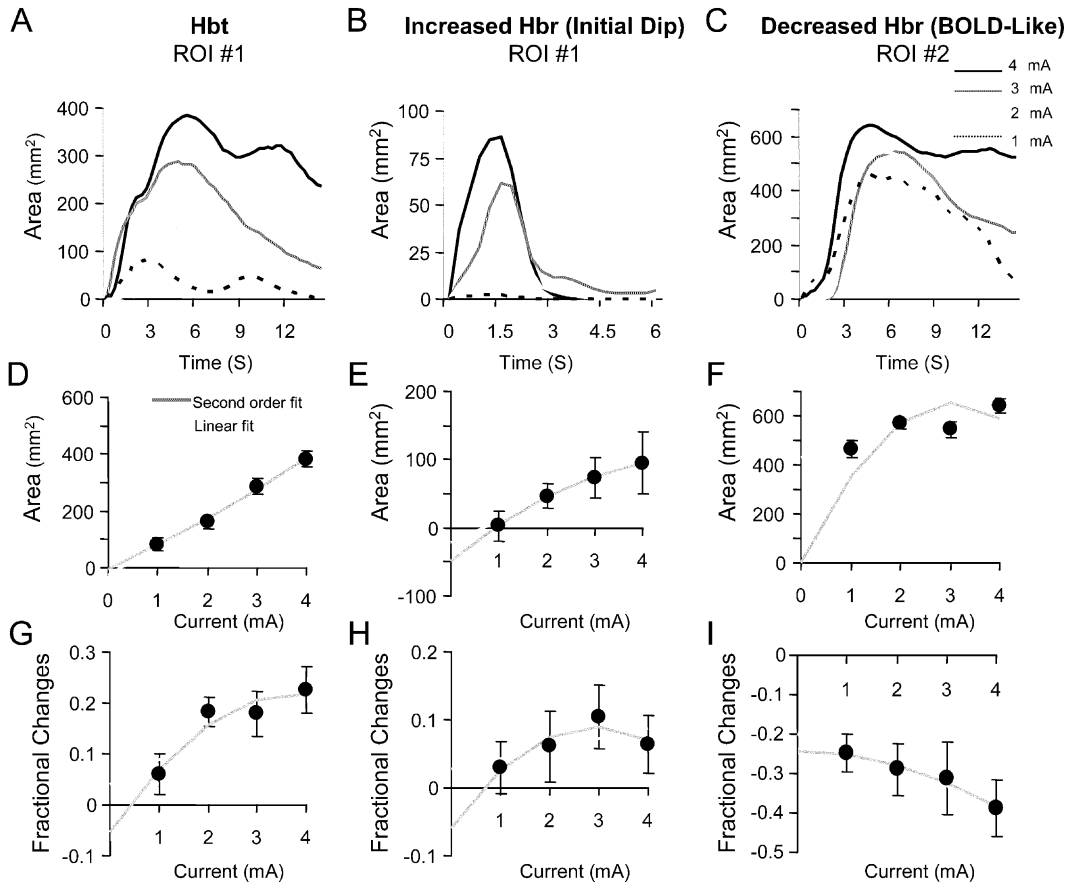

Fig. 5. Time course and relationship between stimulus amplitude and perfusion and oximetry. (A, B, C) Graph of statistically significant pixels of increased Hbt (A), increased Hbr (B), and decreased Hbr (C) activation calculated using the modified Beer–Lambert law. Gray bar marks duration of stimulation. Data are from a different patient than shown in Figs. 1 and 3. (D, E, F) Graph of relationship between stimulus amplitude and maximal area of spread of increased Hbt (D), increased Hbr (E), or decreased Hbr (F). (G, H, I) Graph of relationship between stimulus amplitude and maximal change in increased Hbt (G), increased Hbr (H), or decreased Hbr (I). Note that an increase in stimulus amplitude causes a linear increase in the area of the initial dip and Hbt signals but a nonlinear increase in the BOLD signals and nonlinear increases in percent light change for all signals with a plateau effect.

firmed that tissue oxygen changes parallel the optical data recorded at these wavelengths (Ances, 2004; Thompson et al., 2003, 2004).

We found that, at low levels of cortical stimulation, the initial dip was patchy and inhomogeneous which may explain its elusive nature in other experiments involving physiologic cortical stimulation following normal sensory input. Our laboratory has also found a large dip in hemoglobin oxygenation following both interictal (Suh et al., 2005) and ictal (Bahar et al., 2005) epileptiform events in the rat. Pharmacologically induced seizures, like bipolar stimulation, however, are non-physiologic cortical events which activate large populations of neurons simultaneously. Based on our data, we propose that the ability to detect the initial dip may depend on the magnitude of the cortical stimulus (i.e. degree of synaptic activity). Cortical processing of physiologic sensory stimulation may produce such a small decrease in oxygenation that it is just at the limit of detection with current instruments. Alternatively, a tissue oxygen buffer may mask the initial dip until $CMRO_2$ is high enough (Buxton, 2001; Buxton et al., 1998). Studies in rats using graded hindlimb electrical stimulation have shown that the initial dip was smaller with lower amplitude stimulation (Nemoto et al., 2004; Sheth et al., 2004) and hypothesized that low levels of synaptic activity may not require oxygen extraction from the vasculature (Sheth et al., 2004). Likewise, stimulating the rat whisker physiologically was shown to elicit no dip in one study (Lindauer et al., 2001), while electrical stimulation elicited a graded dip based on the amplitude of stimulation (Jones et al., 2001). In cat visual cortex, single-unit spike rate was found to be directly proportional to the degree of deoxygenation (Thompson et al., 2003). Hence, both epilepsy and bipolar stimulation appear to be useful non-physiologic experimental models for examining the relationship between cortical activity, metabolism, and oxygen utilization since they stress the system into a state of hypermetabolism which may deplete the hypothetical oxygen buffer leading to a supranormal initial dip (Buxton, 2001; Buxton et al., 1998).

The early focal increase in Hbt we recorded in human cortex following bipolar stimulation complements recent experiments in rodent somatosensory cortex and monkey visual cortex that have demonstrated the localization potential of CBV as signal for precise brain mapping (Sheth et al., 2003, 2004; Erinjeri and Woolsey, 2002; Vanzetta et al., 2004). Earlier experiments using ORIS had shown that CBV-based signals correlated less accurately with neuronal activity since the signal is vascular-based and over-compensates for the metabolic demands of the cortex by “watering the garden for the sake of one hungry flower” (Frostig et al., 1990; Malonek and Grinvald, 1996). More recent studies have shown that CBV colocalizes with neuronal activity when measured within the first 1–2 s after the neuronal event (Sheth et al., 2003, 2004)

and when contributions from macrovasculature can be minimized (Vanzetta et al., 2004). The ability to use Hbt (CBV) rather than the initial dip or later decrease in Hbr (BOLD) as a mapping signal may be important for fMRI since the signal-to-noise ratio is higher than for the initial dip and spatial specificity is greater than for the BOLD signal. However, the utility of the CBV signal for mapping functional architecture had always presumed an anatomic relationship between functional architecture (e.g., cortical columns) and penetrating arterioles (Sheth et al., 2004; Woolsey et al., 1996; Vanzetta et al., 2004; Cox et al., 1993). These data were supported by conversion cast studies showing dense capillary networks confined to single barrels in rat neocortex (Cox et al., 1993, Woolsey et al., 1996) and correlations between capillary density and intrinsic optical signals (Harrison et al., 2002). In our study, the region of bipolar stimulation did not overlap with a single cortical column but likely encompassed multiple columns. We have similarly shown that non-columnar epileptiform activity can be localized with the CBV signal (Suh et al., 2005). These data support the existence of CBV and CBF regulation at the level of the capillary in humans and the ability of this signal to map cortical events that do not correspond directly with columnar architecture. Corrosion cast studies in humans demonstrate myocytes and pericytes around arterioles and capillaries which can mediate fine cerebral autoregulation (Reina-De La Torre et al., 1998). Our use of single condition subtraction rather than differential imaging also supports this theory since we did not artificially remove the extent of the signal change.

The relationship between stimulus amplitude and the optical signal has been investigated primarily in rat somatosensory cortex (Devor et al., 2003; Sheth et al., 2003, 2004; Nemoto et al., 2004). Some studies demonstrated that hemodynamic responses increase beyond an electrophysiologic plateau at all wavelengths (Devor et al., 2003). In contrast, others have shown that the oxygen-dependent signals, which vary with anesthetic state and blood gas tension, are nonlinear and less reliable indicators of the degree of neuronal activity compared with CBV-related signals, which are linear within a narrow range (Sheth et al., 2003, 2004; Nemoto et al., 2004). The existence of a tissue oxygen buffer also contributes to nonlinearities since low levels of synaptic activity may not require increases in oxygen extraction (Buxton et al., 1998; Sheth et al., 2004). The relevance of these findings in rat to human brain mapping is unclear. We found a linear relationship between stimulus amplitude and the area of the optical signal for both the initial dip and the CBV, but not BOLD signals. On the other hand, the percent change in reflection of light increased nonlinearly for both the CBV and oximetry signals and then plateaued at high levels of stimulation. These results imply that with increasing stimulation there are hemodynamic changes in progressively larger areas of cortex, possibly reflecting activation of a larger population of neurons, but the hemodynamic effects saturate in any individual area. Presumably, cortical stimulation depolarizes a majority of local neurons, and increasing the stimulus amplitude recruits adjacent neurons rather than depolarizing more neurons locally. This finding in humans may be species-specific. On the other hand, our results in humans may not be as "clean" as laboratory studies in animals since time constraints limit the number of repetitions of each paradigm. We noticed that vasomotor noise in the human, which occurs at 0.1 Hz in the rat (Mayhew et al., 1996), caused a large artifact but at a very irregular and unpredictable frequency, as previously noted (Shoham and Grinvald, 2001). For this reason, all trials with detectable vasomotor noise were eliminated prior to analysis. In addition, we cannot rule out the possibility that patients with epilepsy have abnormal neurovascular coupling compared with normals, although we found similar results when our data were recorded within or adjacent to the epileptic focus.

Our results also have clinical implications. Cortical stimulation mapping has been used for decades to localize functional brain areas during neurosurgical procedures (Ojemann, 1991; Uematsu et al., 1992; Schwartz et al., 1999). The mechanism is presumed to be direct depolarization of cell somata and axons causing local activation (Ranck, 1975). Hence, stimulation of primary areas such as Rolandic or visual cortex causes positive phenomena such as movement, sensation, or the appearance of phosphenes. Direct cortical stimulation in higher order areas, such as language cortex, does not elicit positive phenomena but rather interrupts cortical processing and generally requires much higher amplitude stimulation than in primary areas. The mechanism by which cortical stimulation disrupts cortical processing is not known, but hypotheses include disruption of synaptic activity, desynchronization, and neurotransmitter depletion (Nathan et al., 1993; Haycock et al., 1987). We offer a novel hypothesis for the mechanism whereby stimulation mapping disrupts cortical activity at high amplitudes, namely, transient focal ischemia. The duration of the increase in deoxygenated hemoglobin in our study increased nonlinearly with increasing stimulus amplitude and at the higher amplitudes lasted as long as 6 s following a 2-s stimulation. This delay is consistent with phenomenology and psychophysical responses to cortical stimulation during language mapping since subjects' neuropsychological functions do not return to baseline the instant the stimulation ceases but rather may require several seconds for recovery. Lengthy stimulation at sufficiently high amplitudes could potentially cause permanent damage from ischemic or excitotoxic injury (Yuen et al., 1981). Our results confirm the focality of bipolar cortical stimulation in humans with respect to the initial dip in hemoglobin oxygen, while the late increase in Hbt and late BOLD-related signal was more widespread, often involving adjacent gyri. Thus, we can conclude that it is unlikely that decreases in Hbr or increases in Hbt have a significant effect on human cortical processing since electrical stimulation can interrupt language processing in one 1-cm^2 area of cortex while stimulation in an adjacent 1-cm^2 area leaves language unaffected (Ojemann, 1991).

Acknowledgments

This work was supported by NIH/NINDS grants K08 NS43799 and R21 NS044812, as well as by grants from the CURE and DANA Foundations. We gratefully acknowledge Koon-Ho Danny Wong, Challon Perry, Nina Bowen, and Saadat Shariff for technical assistance and Dr. Jonathan Victor for a proofreading of the manuscript.

References

Ances, B.M., 2004. Coupling of changes in cerebral blood flow with neural activity: what must initially dip must come back up. J. Cereb. Blood Flow Metab. 24 (1), 1–6 (Jan.).

Ances, B.B., Buerk, D.G., Greenberg, J.H., Detre, J.A., 2001. Temporal dynamics of the partial pressure of brain tissue oxygen during

functional forepaw stimulation in rats. Neurosci. Lett. 306 (1–2), 106–110 (Jun. 22).
Bahar, S., Suh, M., Mehta, A., Schwartz, T.H., 2005. In vivo intrinsic optical signal imaging of neocortical epilepsy. In: Broderick, P.A., Rahni, D.N., Kolodny, E.H. (Eds.), Bioimaging in Neurodegeneration 1st ed. Humana Press, Totowa, NJ, pp. 149–175.
Butovas, S., Schwarz, C., 2003. Spatiotemporal effects of microstimulation in rat neocortex: a parametric study using multielectrode recordings. J. Neurophysiol. 90 (5), 3024–3039 (Nov.).
Buxton, R.B., 2001. The elusive initial dip. NeuroImage 13, 953–958.
Buxton, R.B., Wong, E.C., Frank, L.R., 1998. Dynamics of blood flow and oxygenation changes during brain activation: the balloon model. Magn. Res. Med. 39, 855–864.
Cannestra, A.F., Black, K.L., Martin, N.A., Cloughesy, T., Burton, J.S., Rubinstein, E., Woods, R.P., Toga, A.W., 1998. Topographical and temporal specificity of human intraoperative optical intrinsic signals. NeuroReport 9, 2557–2563.
Cannestra, A.F., Pouratian, N., Bookheimer, S.Y., Martin, N.A., Becker, D.P., Toga, A.W., 2001. Temporal spatial differences observed by functional MRI and human intraoperative optical imaging. Cereb. Cortex 11, 773–782.
Cox, S.B., Woolsey, T.A., Rovainen, C.M., 1993. Localized dynamic changes in cortical blood flow with whisker stimulation corresponds to matched vascular and neuronal architecture of rat barrels. J. Cereb. Blood Flow Metab. 13, 899–913.
Creutzfeldt, O.D., Watanabe, S., Lux, H.D., 1966. Relations between EEG phenomena and potentials of single cortical cells. I. Evoked responses after thalamic and epicortical stimulation. Electroencephalogr. Clin. Neurophysiol. 20 (1), 1–18 (Jan.).
Devor, A., Dunn, A.K., Andermann, M.L., Ulbert, I., Boas, D.A., Dale, A.M., 2003. Coupling of total hemoglobin concentration, oxygenation, and neural activity in rat somatosensory cortex. Neuron 39, 353–359.
Erinjeri, J.P., Woolsey, T.A., 2002. Spatial integration of vascular changes with neural activity in mouse cortex. J. Cereb. Blood Flow Metab. 22, 353–360.
Ernst, T., Henning, J., 1994. Observations of a fast response in functional MR. Magn. Res. Med. 32, 146–149.
Forsting, M., Albert, F.K., Kunze, A., Adams, H.P., Zenner, D., Sarto, K., 1993. Extirpation of glioblastomas: MR and CT follow-up of residual tumor and regrowth patterns. AJNR 14, 77–87.
Fox, P.T., Raichle, M.E., 1986. Focal physiological uncoupling of cerebral blood flow and oxidative metabolism during somatosensory stimulation in human subjects. Proc. Natl. Acad. Sci. U. S. A. 83, 1140–1144.
Fox, P.T., Raichle, M.E., Mintun, M.A., Dence, C., 1988. Nonoxidative glucose consumption during focal physiologic neural activity. Science 241, 462–464.
Frannson, P., Kruger, G., Merboldt, K.D., Frahm, J., 1998. Temporal characteristics of oxygenation-sensitive MRI responses to visual activation in humans. Magn. Res. Med. 39, 912–919.
Frostig, R.D., Lieke, E.E., Ts'o, D.Y., Grinvald, A., 1990. Cortical functional architecture and local coupling between neuronal activity and the microcirculation revealed by in vivo high-resolution optical imaging of intrinsic signals. Proc. Natl. Acad. Sci. 87, 6082–6086.
Haglund, M.M., Hochman, D.W., 2004. Optical imaging of epileptiform activity in human neocortex. Epilepsia 45 (S4), 43–47.
Haglund, M.M., Ojemann, G.A., Hochman, D.W., 1992. Optical imaging of epileptiform and functional activity in human cerebral cortex. Nature 358, 668–671.
Harrison, R.V., Harel, N., Panesar, J., Mount, R.J., 2002. Blood capillary distribution correlates with hemodynamic-based functional imaging in cerebral cortex. Cereb. Cortex 12 (3), 225–233.
Haycock, J.W., Levy, W.B., Cotman, C.W., 1987. Stimulation dependent depression of neurostransmitter release in the brain: [Ca] dependence. Brain Res. 155, 192–195.
Hess, A., Stiller, D., Kaulisch, T., Heil, P., Scheich, H., 2000. New insights into the hemodynamic blood oxygenation level-dependent response though combination of functional magnetic resonance imaging and optical recording in gerbil barrel cortex. J. Neurosci. 20, 3328–3338.
Hu, X., Le, T.H., Ugurbil, K., 1997. Evaluation of the early response in fMRI in individual subjects using short stimulus duration. Magn. Res. Med. 37, 877–884.
Jones, M., Berwick, J., Johnston, D., Mayhew, J.E.W., 2001. Concurrent optical imaging spectroscopy and laser-Doppler flowmetry: the relationship between blood flow, oxygenation, and volume in rodent barell cortex. NeuroImage 13, 1002–1015.
Kim, D.-S., Duong, T.Q., Kim, S.-G., 2000. High-resolution mapping of iso-orientation columns by fMRI. Nat. Neurosci. 3, 164–169.
Lindauer, U., Royl, G., Leithner, C., Kuhl, M., Gold, L., Gethman, J., Kohl-Bareis, M., Villringer, A., Dirnagl, U., 2001. No evidence for early decrease in blood oxygenation in rat whisker cortex in response to functional activation. NeuroImage 13, 988–1001.
Logothetis, N.K., Gugenberger, H., Peled, S., Pauls, J., 1999. Functional imaging of the monkey brain. Nat. Neurosci. 2, 555–562.
Malonek, D., Grinvald, A., 1996. Interactions between electrical activity and cortical microcirculation revealed by imaging spectroscopy: implications for functional brain mapping. Science 272, 551–554.
Mandeville, J.B., Marota, J.J., Ayata, C., Moskowitz, M.A., Weisskoff, R.M., Rosen, B.R., 1999. MRI measurement of the temporal evolution of relative CMRO(2) during rat forepaw stimulation. Magn. Res. Med. 42, 944–951.
Mayhew, J.E.W., Askew, S., Zheng, Y., Porrill, J., Westby, G.W.M., Redgrave, P., Rector, D.M., Harper, R.M., 1996. Cerebral vasomotion: a 0.1-Hz oscillation in reflected light imaging of neural activity. NeuroImage 4, 183–193.
Mayhew, J.E.W., Zheng, Y., Hou, Y., Vuksanovic, B., Berwick, J., Askew, S., Coffey, P., 1999. Spectroscopic analysis of changes in remitted illumination: the response to increased neural activity in brain. NeuroImage 10, 304–326.
Mayhew, J.E.W., Johnston, D., Berwixk, J., Jones, M., Cofey, P., Zheng, Y., 2000. Spectroscopic analysis of neural activity in brain: increased oxygen consumption following activation of barrel cortex. NeuroImage 12, 664–675.
Menon, R.S., Ogawa, S., Hu, X., Strupp, J.P., Anderson, P., Ugurbil, K., 1995. BOLD based functional MRI at 4 Tesla includes a capillary bed contribution: echo-planar imaging correlates with previous optical imaging using intrinsic signals. Magn. Res. Med. 33, 453–459.
Nathan, S.S., Sinha, S.R., Gordon, B., Lesser, R.P., Thakor, N.V., 1993. Determination of current density distributions generated by electrical stimulation of the human cerebral cortex. Electroencephalogr. Clin. Neurophysiol. 86 (3), 183–192.
Nemoto, M., Nomura, Y., Sato, C., Tamura, M., Houkin, K., Koyanagi, I., Abe, H., 1999. Analysis of optical signals evoked by peripheral nerve stimulation in rat somatosensory cortex: dynamic changes in hemoglobin concentration and oxygenation. J. Cereb. Blood Flow Metab. 19, 246–259.
Nemoto, M., Sheth, S., Guiou, M., Pouratian, N., Chen, J.W.Y., Toga, A.W., 2004. Functional signal- and paradigm-dependent linear relationships between synaptic activity and hemodynamic responses in rat somatosensory cortex. J. Neurosci. 24, 3850–3861.
Ogawa, S., Lee, T.M., Kay, A.R., Tank, D.W., 1990. Brain magnetic resonance imaging with contrast dependent on blood oxygenation. Proc. Natl. Acad. Sci. U. S. A. 87, 9868–9872.
Ojemann, G.A., 1991. Cortical organization of language. J. Neurosci. 11, 2281–2287.
Pouratian, N., Sicotte, N., Rex, D., Marin, N.A., Becker, D.P., Cannestra, A.F., Toga, A.W., 2003. Spatial/temporal correlation of BOLD and optical intrinsic signals in human. Magn. Res. Med. 47, 766–776.
Ranck, J.B., 1975. Which elements are excited in electrical stimulation of mammalian central nervous system: a review. Brain Res. 98, 417–440.
Ratzlaff, E.H., Grinvald, A., 1991. A tandem-lens epifluorescence macroscope: hundred-fold brightness advantage for wide field imaging. J. Neurosci. Methods 36, 127–137.

Reina-De La Torre, F., Rodriguez-Baeza, A., Sahuquillo-Barris, J., 1998. Morphological characteristics and distribution pattern of the arterial vessels in human cerebral cortex: a scanning electron microscope study. Anat. Rec. 251, 87–96.

Roy, C., Sherrington, C., 1890. On the regulation of the blood supply to the brain. J. Physiol. (London) 11, 85–108.

Sato, K., Nariai, T., Sasaki, S., Yazawa, I., Mochida, H., Miyakawa, N., Momose-Sato, Y., Kamino, K.Y.O., Hirakawa, K., Ohno, K., 2002a. Intraoperative intrinsic signal imaging of neuronal activity from subdivisions of the human primary somatosensory cortex. Cereb. Cortex 12, 269–280.

Sato, C., Nemoto, M., Tamura, M., 2002b. Reassessment of activity-related optical signals in somatosensory cortex by an algorithm with wavelength-dependent path length. Jpn. J. Physiol. 52, 301–312.

Schwartz, T.H., Devinsky, O., Doyle, W., Perrine, K., 1999. Function-specific high-probability nodes identified in posterior language cortex. Epilepsia 40, 575–583.

Schwartz, T.H., Chen, L.M., Friedman, R.M., Spencer, D.D., Roe, A.W., 2004. Intraoperative optical imaging of human face cortical topography: a case study. Neuroreport 15 (9), 1527–1531 (Jun. 28).

Sheth, S.A., Nemoto, M., Guiuo, M., Walker, M., Pouratian, N., Toga, A.W., 2003. Evaluation of coupling between optical intrinsic signals and neuronal activity in rat somatosensory cortex. NeuroImage 19, 884–894.

Sheth, S.A., Nemoto, M., Guiou, G., Walker, M., Pouratian, N., Heagemann, N., Toga, A.W., 2004. Columnar specificity of microvascular oxygenation and volume responses: implications for functional brain mapping. J. Neurosci. 24.

Shoham, D., Grinvald, A., 2001. The cortical representation of the hand in macaque and human area S-1: high resolution optical imaging. J. Neurosci. 21 (17), 6820–6835.

Silva, A.C., Lee, S.P., Iadecola, C., Kim, S.G., 2000. Early temporal characteristics of cerebral blood flow and deoxyhemoglobin changes during somatosensory stimulation. J. Cereb. Blood Flow Metab. 20, 201–206.

Suh, M., Bahar, S., Mehta, A.D., Schwartz, T.H., 2005. Temporal dependence in uncoupling of blood volume and oxygenation during interictal epileptiform events in rat neocortex. J. Neurosci. 25 (1), 68–77.

Thompson, J.K., Peterson, M.R., Freeman, R.D., 2003. Single-neuron activity and tissue oxygenation in the cerebral cortex. Science 14 (299), 1070–1072.

Thompson, J.K., Peterson, M.R., Freeman, R.D., 2004. High-resolution neurometabolic coupling revealed by focal activation of visual neurons. Nat Neurosci. 7 (9), 919–920 (Sep.).

Uematsu, S., Lesser, R., Fisher, R.S., Gordon, B., Hara, K., Krauss, G.L., Vining, E.P., Webber, R.W., 1992. Motor and sensory cortex in human: topography studied with chronic subdural stimulation. Neurosurgery 31, 59–72.

Vanzetta, I., Grinvald, A., 1999. Increased cortical oxidative metabolism due to sensory stimulation: implications for functional brain imaging. Science 286, 1555–1558.

Vanzetta, I., Grinvald, A., 2001. Evidence and lack of evidence for the initial dip in the anesthetized rat: implications for human functional brain imaging. NeuroImage 13, 959–967.

Vanzetta, I., Slovin, H., Omer, D.B., Grinvald, A., 2004. Columnar resolution of blood volume and oximetry functional maps in the behaving monkey: implications for fMRI. Neuron 42, 843–854.

Woolsey, T.A., Rovainene, C.M., Cox, S.B., Henegar, M.H., Liang, G.E., Liu, D., Moskalento, Y.E., Sui, J., Wei, L., 1996. Neuronal units linked to microvascular modules in cerebral cortex: response elements for imaging the brain. Cereb. Cortex 6, 647–660.

Yuen, T.G.H., Agnew, W.F., Bullara, L.A., Jacques, S., McCreery, D.B., 1981. Histological evaluation of neural damage from electrical stimulation: considerations for the selection of parameters for clinical application. Neurosurgery 9, 292–299.